Synthesis of 3-Arylpiperazinylalkylpyrrolo[3,2-*d*]pyrimidine-2,4-dione Derivatives as Novel, Potent, and Selective α_1-Adrenoceptor Ligands‡

Emanuele Patanè,§ Valeria Pittalà,*,§ Francesco Guerrera,§ Loredana Salerno,§ Giuseppe Romeo,§ Maria Angela Siracusa,§ Filippo Russo,§ Fabrizio Manetti,# Maurizio Botta,# Ilario Mereghetti,† Alfredo Cagnotto,† and Tiziana Mennini†

Dipartimento di Scienze Farmaceutiche, Università di Catania, viale A. Doria 6, 95125 Catania, Italy, Istituto di Ricerche Farmacologiche "Mario Negri", via Eritrea 62, 20157 Milano, Italy, and Dipartimento Farmaco Chimico Tecnologico, Università degli Studi di Siena, via A. Moro, 53100 Siena, Italy

Received August 2, 2004

Novel compounds characterized by a pyrrolo[3,2-*d*]pyrimidine-2,4-dione (PPm) system connected through an alkyl chain to a phenylpiperazine (PPz) residue were designed as structural analogues of the α_1-adrenoceptor (α_1-AR) ligand RN5 (**1**). In this new series of derivatives an arylpyrrolo moiety has replaced the indole nucleus of RN5. Several structural modifications were performed on the PPm and PPz moieties and the connecting alkyl chain. These compounds were synthesized and tested in radioligand binding experiments where many of them showed interesting binding profiles. Some compounds, including **31**, **34**, and **36**, displayed substantial α_1-AR selectivity with respect to serotoninergic 5-HT_{1A} and dopaminergic D_1 and D_2 receptors. Two different molecular modeling approaches (pharmacophoric mapping and quantitative structure−affinity relationship analysis) have been applied to rationalize, at a quantitative level, the relationships between affinity toward α_1-ARs and the structure of the studied compounds. Several QSAR models have been reported and described, accounting for the influence of various molecular portions on such affinity data.

Introduction

The adrenoceptors (ARs) mediate the functional effects of catecholamines such as adrenaline and noradrenaline, playing important roles in the control of blood pressure, myocardial contractile rate and force, airway reactivity, and a variety of metabolic functions.[1,2]

The ARs are divided into three principal families: α_1, α_2, and β; all ARs are members of the superfamily of G-protein-coupled receptors that transduce signal across the cell membrane, thus initiating a variety of intracellular biochemical events.[1,2] The α_1-ARs are presently classified into three subtypes designated as α_{1A}, α_{1B}, α_{1D} and having high affinity for prazosin.[3−5] In addition, another subtype (α_{1L}) has been proposed;[6,7] this is characterized by low affinity for prazosin, but efforts to clone it are still unsuccessful. The α_1-ARs play a central role in the maintenance of smooth muscle tone in both the cardiovascular system and the prostate; drugs interacting with the α_1-ARs are widely used in the treatment of some diseases, including hypertension and benign prostatic hyperplasia (BPH).[8,9]

Although in the past years pharmaceutical research has focused the attention on the development of subtype-selective ligands,[10] comparable efforts have been made to discover ligands selective for α_1-ARs over other related receptors, such as the serotoninergic 5-HT_{1A} (showing 45% of structural similarity) and the dopaminergic D_1 and D_2 receptors.[11−13] Among the compounds showing high affinity toward α_1-ARs, relevant attention has been devoted to molecules containing an arylpiperazinyl moiety as the pharmacophoric portion.[12−16]

Chart 1

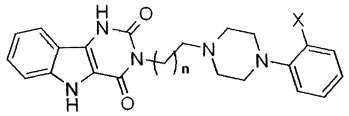

1: X = OCH_3, n = 1
2: X = Cl, n = 1
3: X = OCH_3, n = 2

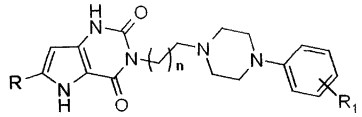

21-40

In the course of our studies in the field of new and selective α_1-AR ligands, we have previously described a class of pyrimido[5,4-*b*]indole-2,4-diones having an arylpiperazinylalkyl chain at position 3 (Chart 1).[17] Some of these compounds showed high affinity for α_1-ARs and good selectivity over the 5-HT_{1A} receptors. In particular RN5 (**1**), in which X is a methoxy group, displayed the highest affinity, and compound **2**, in which X is a chlorine, showed a high level of selectivity. More recently, some thienopyrimidine-2,4-dione derivatives related to indole compounds have been described in a patent and claimed as α_1-AR ligands selective for α_{1D} with respect to α_{1A} and α_{1B} receptors.[18]

‡ This paper is dedicated to the memory of Dr. Emanuele Patanè.

* To whom correspondence should be addressed. Phone: +39 095 7384273. Fax: +39 095 222239. E-mail: vpittala@unict.it.
§ Università di Catania.
# Università degli Studi di Siena.
† Istituto di Ricerche Farmacologiche "Mario Negri".

10.1021/jm040870h CCC: $30.25
Published on Web 02/25/2005

Scheme 1[a]

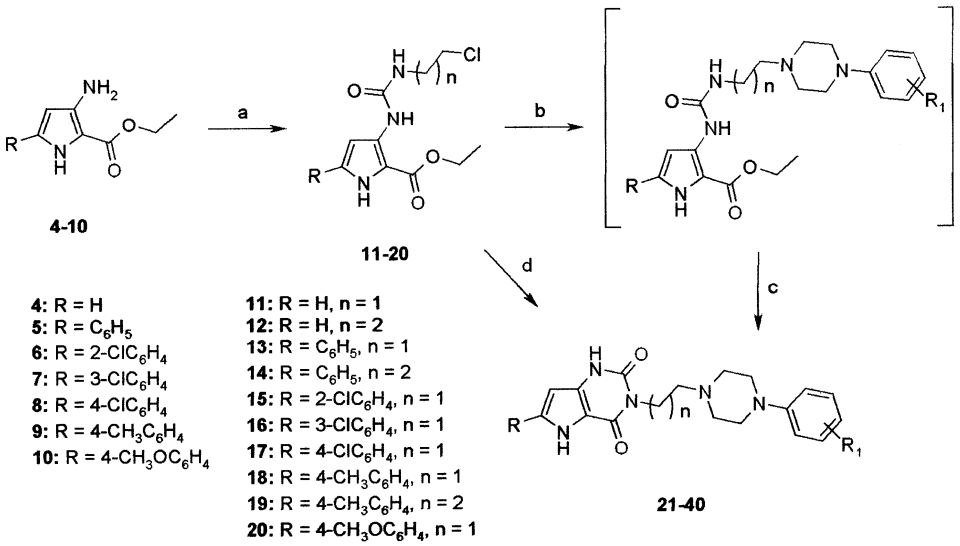

[a] Conditions: (a) $ClCH_2(CH_2)_nNCO$, toluene, reflux; (b) 1-(substituted phenyl)piperazine, $NaHCO_3$, NaI, THF, reflux; (c) KOH/MeOH, reflux; (d) 1-(2-substituted phenyl)piperazine, 140 °C.

With the aim to obtain highly selective α_1-AR ligands over other related receptors, in this paper we describe the synthesis and the binding data for α_1-ARs and 5-HT_{1A}, D_1, D_2 receptors of a series of new 3-arylpiperazinylalkylpyrrolo[3,2-*d*]pyrimidine-2,4-dione derivatives (**21**−**40**) (Chart 1) in which an arylpyrrolo moiety has replaced the indole nucleus in the structures of compounds **1** and **2**. In the new molecules, the aryl ring, which is not condensed to form a planar tricyclic system, is linked to the 6-position of the pyrrolo[3,2-*d*]pyrimidine-2,4-dione (PPm) moiety and bears substituents of different nature in the various positions. As in **1** and **2**, the PPm moiety is linked, through an alkyl chain, to a phenylpiperazine (PPz) substructure bearing a methoxy or a chloro substituent at the 2-position of the phenyl ring.

New compounds were evaluated for their ability to fit a pharmacophoric model for α_1-AR antagonists previously built by our research group and constituted by five features representing three hydrophobic regions (hereafter referred to as HY1−3 features), a hydrogen bond acceptor (HBA), and a positively ionizable group (PI).[12] The model was able to predict affinity values of 6-unsubstituted (**21**−**24**), 6-phenyl (**25**−**29**), and 6-(2-chlorophenyl) (**30**, **31**) derivatives, in good agreement with their corresponding experimental data. However, the affinity of compounds **32**−**40**, characterized by a substituent at the meta or para position of the 6-phenyl ring, was mispredicted. This was mainly due to the fact that the pharmacophoric model was unable to account for the influence of such a substituent on affinity. In fact, substituents at the 3- or 4-position of the 6-phenyl ring lie in an empty region of space, where any of the pharmacophoric features was located. As a consequence of this predictive limitation of the model, we have pursued an alternative approach aimed at analyzing how affinity values were correlated with structural properties of the studied compounds. For this purpose, we have applied the genetic function approximation (GFA)[19,20] to generate multiple QSAR equations able to describe the affinity in terms of molecular descriptors. As a result, affinity values were found to be dependent on contributions from methylene groups, chlorine substituents, oxygen atoms as in the methoxy groups, molecular refractivity, and positive and negative charge surface areas.

Chemistry

The synthetic route to the pyrrolo[3,2-*d*]pyrimidine-2,4-dione derivatives is described in Scheme 1. The starting 3-amino-1*H*-pyrrole-2-carboxylic acid ethyl ester **4** was prepared utilizing the procedure described by Furneaux et al.[21] Compounds **5**−**8** and **10** were synthesized using substituted benzoyl acetonitriles as starting material, as described by Chen et al.[22−24] The same synthetic method was used to obtain compound **9**, which is not reported in the literature.

Suitable pyrrolo amino esters (**4**−**10**) were reacted with the appropriate chloroalkyl isocyanate in refluxing toluene to give the (chloroalkyl)ureas (**11**−**20**). The obtained ureas were then reacted with suitable 1-(2-substituted phenyl)piperazine hydrochloride in THF in the presence of NaI and $NaHCO_3$ [17] to afford intermediate ureas that, without isolation, were converted into final products **21**−**40** in methanolic sodium hydroxide (method A). Alternatively, some final derivatives were prepared by reacting the appropriate (chloroalkyl)urea derivative at 140 °C for 2 h with a large excess of the suitable 1-(2-substituted phenyl)piperazine in the absence of solvent (method B).[17]

Results and Discussion

SAR Studies. The affinities and selectivities of compounds **21**−**40** for α_1-ARs and related receptors are shown in Table 1. For the derivatives that showed the highest affinity and selectivity toward α_1-ARs over the 5-HT_{1A} receptors, the affinity for dopaminergic D_1 and D_2 receptors was also evaluated. The values are expressed as K_i (nM) values; RN5 (**1**) and **2** were selected as reference substances.

Affinity data clearly showed that most of new synthesized compounds were characterized by very interesting binding profiles. In fact, with the exception of

Table 1. Binding Properties of 3-Arylpiperazinylalkylpyrrolo[3,2-*d*]pyrimidine-2,4-dione Derivatives

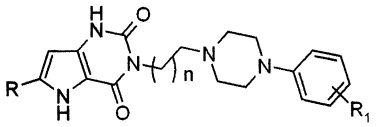

21-40

					K_i (nM)[a]						
compd	method	*n*	R	R_1	α_1	5-HT_{1A}	D_1	D_2	5-HT_{1A}/α_1[b]	D_1/α_1[b]	D_2/α_1[b]
21	A	1	H	2-CH_3O	2.31 ± 0.22	650.6 ± 109.1	ND	ND	282		
22	A	1	H	2-Cl	0.94 ± 0.04	558.5 ± 124.1	>10000	322.1 ± 48.3	594	>10000	343
23	A	2	H	2-CH_3O	28.01 ± 3.76	192.9 ± 30.9	ND	ND	6.9		
24	A	2	H	2-Cl	59.78 ± 8.56	376.2 ± 68.8	ND	ND	6.3		
25	B	1	C_6H_5	2-CH_3O	0.52 ± 0.05	24.01 ± 4.03	ND	ND	46		
26	B	1	C_6H_5	2-Cl	1.08 ± 0.08	35.01 ± 7.05	ND	ND	32		
27	A	2	C_6H_5	2-CH_3O	1.23 ± 0.11	22.36 ± 5.02	ND	ND	18		
28	A	2	C_6H_5	2-Cl	62.37 ± 3.99	129.8 ± 9.8	ND	ND	2.1		
29	B	1	C_6H_5	4-CH_3O	>10000	>10000	ND	ND			
30	B	1	2-ClC_6H_4	2-CH_3O	0.76 ± 0.09	16.14 ± 1.41	ND	ND	21		
31	A	1	2-ClC_6H_4	2-Cl	0.46 ± 0.09	>10000	>10000	27.79 ± 3.89	>20000	>20000	60
32	B	1	3-ClC_6H_4	2-CH_3O	19.32 ± 1.80	16.90 ± 3.02	ND	ND	0.87		
33	B	1	4-ClC_6H_4	2-CH_3O	7.68 ± 1.63	>10000	>10000	3.64 ± 0.63	>1000	>1000	0.47
34	B	1	4-ClC_6H_4	2-Cl	11.70 ± 2.17	>10000	>10000	>10000	>800	>800	>800
35	B	1	4-$CH_3C_6H_4$	2-CH_3O	2.05 ± 0.33	>10000	>10000	19.95 ± 1.51	>4500	>4500	9.7
36	B	1	4-$CH_3C_6H_4$	2-Cl	17.26 ± 4.14	>10000	>10000	>10000	>500	>500	>500
37	A	2	4-$CH_3C_6H_4$	2-CH_3O	47.88 ± 2.80	82.99 ± 23.30	ND	ND	1.73		
38	A	2	4-$CH_3C_6H_4$	2-Cl	110.1 ± 11.7	>10000	ND	ND	>90		
39	A	1	4-$CH_3OC_6H_4$	2-CH_3O	0.77 ± 0.10	525.5 ± 94.1	>10000	2.11 ± 0.35	682	>10000	2.74
40	A	1	4-$CH_3OC_6H_4$	2-Cl	3.40 ± 0.54	>10000	>10000	2.23 ± 0.42	>2500	>2500	0.65
1[c]					0.21 ± 0.02	50.00 ± 4.70			238		
2[c]					0.53 ± 0.18	>10000			>15000		

[a] K_i values were calculated as described in the Experimental Section and are the mean ± SD of three separate experiments. [b] Ratio between K_i(5-HT_{1A})/$K_i(\alpha_1)$, $K_i(D_1)/K_i(\alpha_1)$, and $K_i(D_2)/K_i(\alpha_1)$. [c] Data taken from ref 17.

compound **29**, they exhibited good affinity toward α_1-ARs (some of them in the subnanomolar range) and selectivity over the other tested receptors.

Because our first aim was to verify whether the indole moiety of pyrimido[5,4-*b*]indole-2,4-diones could be replaced by an arylpyrrole scaffold, first we synthesized the 6-phenylpyrrolo[3,2-*d*]pyrimidine-2,4-dione derivatives **25**−**28**, more structurally related to **1** and **2**. Compounds **25** and **26** showed affinity toward α_1-ARs (K_i = 0.52 and 1.08 nM, respectively) in the same range as **1** and **2** showed (K_i = 0.21 and 0.53 nM, respectively), indicating that the pyrrole moiety is a good replacement for the indole residue. These results encouraged us to carry out additional modifications to improve both affinity and selectivity. We then synthesized compounds **33**−**40** characterized by the presence of substituents, such as chlorine, methyl, or methoxy, at the 4-position of phenyl ring linked to PPm. As a general trend, these substitutions afforded compounds showing a slight decrease in affinity for α_1-ARs with respect to compounds **25** and **26** but, with exception of **37**, with an enhanced selectivity over the other receptors. In particular, compounds **35** and **39** showed the highest affinity for α_1-ARs (K_i = 2.05 and 0.77 nM, respectively), whereas compounds **34** and **36** were noteworthy for their selectivity over all the other tested receptors (K_i for 5-HT_{1A}, D_1, and D_2 receptors greater than 10 000 nM). These results indicate that the presence of a substituent at the 4-position of the phenyl ring linked to PPm, although not essential for the affinity at α_1-ARs, can be critical to discriminate between α_1-ARs and all the other tested receptors. To investigate the effect of the shift of the substituent on the phenyl ring from the 4-position to the 3 and 2 positions, we selected 4-chloroderivative **34** and synthesized 3-chloro **32** and 2-chloro **30** and **31** substituted analogues. Compound **32** showed a slight decrease in affinity for α_1-ARs with a dramatic loss of selectivity, whereas compounds **30** and **31** showed an increase in affinity for α_1-ARs (K_i = 0.76 and 0.46 nM, respectively). Moreover, **31** displays an interesting selectivity profile because it showed no affinity for the 5-HT_{1A} and D_1 receptors (5-HT_{1A}/α_1 and D_1/α_1 greater than 20 000 nM) and only a moderate K_i value at the D_2 receptor (D_2/α_1 = 60).

With the aim of investigating the role of the phenyl ring linked to PPm, we synthesized compounds **21**−**24** in which this ring was removed. In binding assays these compounds showed lower affinity for α_1-ARs (compare **21** with **25**, **23** with **27**, and **24** with **28**) with the exception of **22** whose affinity and selectivity were notable (K_i = 0.94 nM, 5-HT_{1A}/α_1 = 594, $D_1/\alpha_1 \geq 10\,000$, D_2/α_1 = 343).

Several α_1-AR or 5-HT_{1A} ligands reported in the literature present a PPz moiety located at a different distance from a second structural portion, generally represented by a heterocyclic ring or system, containing an amide group.[13,25,26] The length of the alkyl chain connecting these two substructures greatly influences affinity and selectivity of such ligands. Compounds **23**, **24**, **27**, **28**, **37**, and **38** were synthesized to evaluate the influence of a propylene instead of an ethylene chain on α_1-AR affinity. Binding data clearly demonstrate that the lengthening of this connecting chain determines a general loss in both affinity and selectivity for α_1-ARs.

The effects of the nature and the position of substituents on the phenyl ring of the PPz moiety have been extensively studied in many PPz-based α_1-AR ligands.[12−16] As previously reported (and confirmed in this

series by the binding data of compound **29**), a substituent in the 4-position of the aryl ring generally leads to compounds with much lower affinity.[17,27,28] On the other hand, substituents in the 2-position usually give ligands with higher affinity. Considering these premises and the structures of compounds **1** and **2**, we prepared and evaluated 2-methoxy- or 2-chlorophenylpiperazinyl derivatives. According to the trend previously encountered in the pyrimido[5,4-*b*]indole-2,4-dione series,[17] 2-methoxy substitution gave products with the highest affinity on α_1-ARs (**25**, **30**, and **39**) whereas 2-chloro substitution gave products with lower affinity for α_1-ARs but are extremely selective because they are almost inactive on the other tested receptors, particularly on 5-HT_{1A} (**22**, **34**, **36**, and **40**).

Molecular Modeling Calculations. 1. Superposition to a Pharmacophoric Model for α_1-Adrenoceptor Antagonists. An additional effort to rationalize the relationships between the structure of the new compounds and their biological activity was performed by analyzing the superposition pathways of such compounds onto a pharmacophore model previously developed by us for α_1-adrenoceptor antagonists.[12] In principle, with the exception of **29**, all the compounds were characterized by chemical features able to fill the five features of the pharmacophore. Regarding their orientation with respect to the pharmacophore, the new compounds showed a great similarity with RN5, which constituted an element of the training set used to generate the pharmacophore itself. In detail, the 2-methoxy or 2-chlorophenylpiperazinyl moiety of the inhibitors matched the HY1−HY2−PI system of the pharmacophore, as depicted in Figure 1 for compounds **21**, **25**, and **30**, taken as representative examples of the whole set of the new compounds. Moreover, one of the carbonyl groups of the dione system corresponded to the hydrogen bond acceptor group. In particular, the carbonyl group at the 4-position of the PPm system was more frequently found as the hydrogen bond acceptor. However, because of a 180° rotation of the bicyclic moiety, the carbonyl group at position 2 was sometimes allowed to interact with HBA. Finally, different chemical substituents were found to be able to fill the HY3 feature, allowing the classification of the compounds into three subsets. (i) The first subset was constituted by compounds lacking any substituent at the pyrrole nucleus (i.e., **21**−**24**), able to fill HY3 with the CH−CH system at positions 6 and 7 of the pyrrole ring (Figure 1A). As a consequence of the high fit between such compounds and the pharmacophore model, affinity values were predicted that were in agreement with experimental data. As an example, the pharmacophore model predicted an affinity of 2.0 nM for compound **21**, comparable with the experimental value of 2.3 nM. (ii) The second subset includes compounds **25**−**28**, bearing an unsubstituted phenyl group at the 6-position of the PPm system, which was located inside HY3 (Figure 1B). Compounds **25** and **26** showed an enhanced fit with respect to the corresponding unsubstituted counterparts **21** and **22**, with a consequent improvement of the predicted affinity. Compound **25** was predicted to have an affinity of 0.30 nM, in good agreement with the experimental value of 0.52 nM. (iii) Compounds with a 2-chlorophenyl group at the 6-position of the PPm moiety (namely, **30** and **31**) showed a conformational rearrangement with respect to the 6-phenyl derivatives, allowing superposition of the chlorine atom into the HY3 feature (Figure 1C). Also in this case, the pharmacophore model predicted affinity values well, for example, the predicted affinity of **30** being 0.75 nM, which is comparable with the experimental value of 0.76 nM.

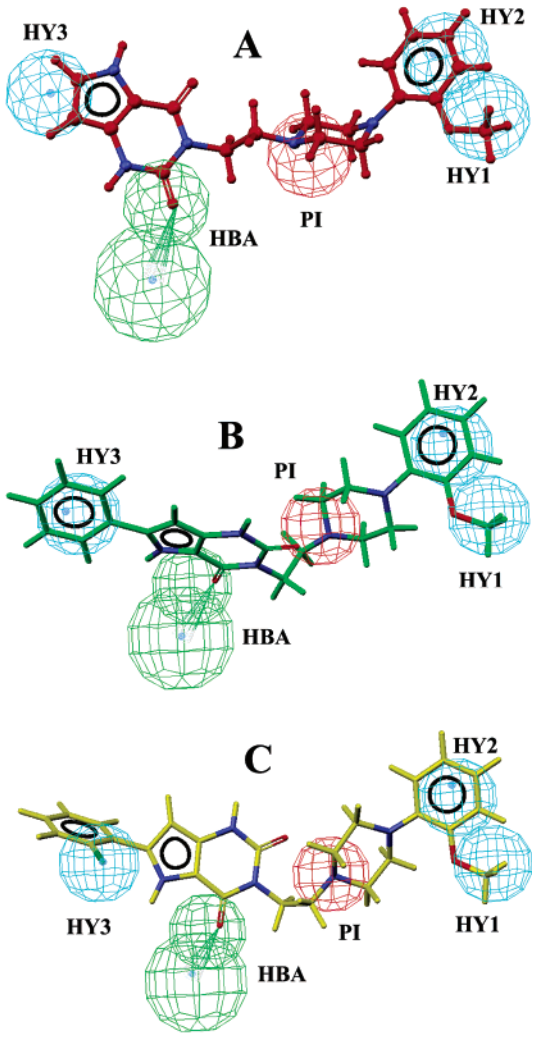

Figure 1. Superposition pattern of compounds **21**, **25**, and **30** into the pharmacophoric model for α_1-AR antagonists. Similar orientations of the *o*-methoxyphenylpiperazine systems were found that were able to fill the HY1−2 features with the substituted phenyl ring and the positive ionizable group PI with the most basic nitrogen atom of the piperazine ring. Moreover, one of the two carbonyl groups at the terminal heterocyclic portion corresponded to the hydrogen bond acceptor group (HBA). In particular, HBA is represented by the carbonyl at the 2-position of compound **21** (A), different from compounds **25** (B) and **30** (C) where the same pharmacophoric feature was the carbonyl at the 4-position. The major difference was found in the region corresponding to HY3. In fact, compound **21** partially matched the hydrophobic sphere with the distal portion of the PPm fragment (that is, the C6−C7 sequence of the pirrole nucleus). Moreover, while the unsubstituted phenyl ring at the 6-position perfectly corresponded to HY3 for compound **25**, its 2-chloro derivative **30** fulfilled the same feature with the halo substituent. Pharmacophoric features are color coded as follows: blue for hydrophobics (HY1−3), red for positive ionizable groups (PI), and green for hydrogen bond acceptors (HBA).

Binding data showed that elongation of the ethyl spacer (linking the PPz and the PPm portions) to a

propyl chain led to a marked decrease in affinity, also accounted for by the pharmacophore model. In fact, the ethyl chain seemed to be the optimal spacer to bring the PPz system at the proper distance from the PPm moiety to allow interactions with all the pharmacophoric features. In contrast, lengthening of the spacer made the superposition into the pharmacophore model more difficult for the compounds. Consequently, only conformers at higher energy (i.e., with a stressed piperazine ring or partially eclipsed Csp^3-Csp^3 systems) were found to be able to partially fill the features of the pharmacophore. Since the two variables (high energy with respect to the minimum and a partial fit onto the pharmacophore) were taken into account by the software to predict affinity values, the last was calculated to be 1−2 orders of magnitude lower with respect to the values of the corresponding ethyl counterparts, in good agreement with experimental data showing a drop in affinity from an ethyl to a propyl spacer. As an example, the affinity of compound **28** was predicted to be 20 nM (versus an experimental value of 62 nM) with respect to the affinity of 0.66 nM (versus an experimental value of 1.1 nM) predicted for the corresponding ethyl derivative **26**.

All the remaining compounds (**32**−**40**) bearing a 3-chlorophenyl or a 4-substituted phenyl ring at the 6-position of the PPm system could also be included in the second subset, since their phenyl ring was usually located inside the HY3 feature of the pharmacophore. However, such compounds were characterized by an additional group (at the 3- or 4-position of the phenyl ring) that lies in an empty region of space where no pharmacophoric feature was located. As a consequence, the pharmacophore model was completely unable to account for variations in affinity, if any, due to the presence of such substituents. As an example, the predicted activity for **33** was 0.45 nM, comparable to the affinity predicted for compound **25** bearing an unsubstituted phenyl ring.

2. QSAR Calculation by Means of the Genetic Function Approximation (GFA). In an effort to overcome the limitation of the pharmacophore model in estimating the affinity of compounds such as **32**−**40** and to produce improved theoretical models able to rationalize at the quantitative level the relationships between affinity data and structural properties of the new compounds, we have applied the genetic function approximation (GFA) algorithm[19,20] as implemented in the Cerius^2 software.[29] GFA has been largely applied in recent years mainly because of its advantages over other traditional multiple regression methods (i.e., it offers a nonlinear approach to generate QSAR models using different basis functions including spline terms and produces multiple QSAR models rather than the usual single model), and the robustness of this statistical technique has been demonstrated by a large number of literature reports also in the field of medicinal chemistry (further details about GFA and its application can be found on the Accelrys Web site, http://www.accelrys.com/doc/life/cerius48/qsar/Output/stat_gfa_nf.html and in recent literature).[30−33]

From the original set of 20 molecules, compound **29**, with undefined affinity, was not included in GFA calculations. The remaining 19 compounds were divided into a training set (14 compounds) and a test set (5 compounds), while their biological activity was used in terms of $-\log K_i$ to have a (better) normal distribution of biological data with respect to values expressed as nanomolar concentrations. The pharmacophoric model previously built for α_1-AR antagonists was used as a tool to perform molecular alignment, that is, to identify (among all the conformers found) the best fitting conformer for each molecule. In detail, each compound was superposed to the pharmacophore by application of the Best Fit option within the Compare/Fit menu of Catalyst.[29] As a result, the conformer chosen for each compound was found to be oriented within the pharmacophore in such a manner that the PPz moiety matched HY1−HY2−PI and the oxygen atom of the carbonyl group at the 4-position represented the HBA feature. Finally, the PPm fragment and its phenyl substituent at the 6-position were the molecular portions filling HY3. Such an alignment was exported by using the Export Workbench Alignments of Catalyst; the partial atomic charges were calculated for each compound by means of the Mopac software implemented in the InsightII package,[29] and charged compounds were imported in Cerius^2 for QSAR calculations. The original set of descriptors (belonging to the classes of topological, spatial, structural, thermodynamic, electronic, and electrotopological state keys) calculated for each compound was pruned in order to avoid the presence of collinear regressors (descriptors) that could return inaccurate results from a statistical point of view. For this purpose, the correlation matrix was investigated to check the linearity between variables (expressed as Pearson's correlation coefficient) and a cutoff of 0.7 was set to discard molecular descriptors affected by collinearity. As a consequence, the final set of descriptors used to generate QSAR models was constituted by 21 variables listed in Table 2.

The GFA algorithm is based on a genetic algorithm to perform a search on the space of possible QSAR equations and uses LOF (lack of fit) as the scoring function to estimate the fitness of each model built. GFA was applied to 21 descriptors, fixing to 100 the population size (the number of QSAR models to be initially generated by a random choice of descriptors). In the models, only linear polynomial terms were allowed, avoiding spline or quadratic terms, to better interpret the final QSAR equations. A large number of crossover operations (20 000) was chosen to generate progeny models that were scored by the LOF parameter to produce the 100 final QSAR models. As a result, all the models constituting the final population possessed roughly the same statistical parameters but each equation may be able to provide different insights to rationalize binding affinity data on the basis of each descriptor participating in the equation itself. Table 3 reports a summary of the eight best final GFA models scored by increasing LOF. The best QSAR model generated from 21 descriptors was chosen on the basis of its lowest LOF value with respect to the other models characterized by comparable statistical parameters (in terms of r^2, internal CV r^2,[34] and F values). It was characterized by an r^2 of 0.920 and an LOF of 0.201. Analysis of the best eight models allowed us to relate molecular descriptors to the affinity values. In detail, affinity de-

Table 2. Summary of the 21 Molecular Descriptors Used To Generate the QSAR Models

no.	descriptor[a]	type	description
1	MR	Thermodynamic	Molar refractivity
2	Density	Spatial	Molecular density
3	PMI-mag	Spatial	Principal moment of inertia
4	Dipole-mag	Electronic	Dipole moment
5	HOMO	Electronic	Highest occupied molecular orbital energy
6	LUMO	Electronic	Lowest unoccupied molecular orbital energy
7	Sr	Electronic	Superdelocalizability
8	Jurs-RPCG	Spatial	Relative positive charge
9	Jurs-RNCG	Spatial	Relative negative charge
10	Jurs-RPCS	Spatial	Relative positive charge surface area
11	Jurs-RNCS	Spatial	Relative negative charge surface area
12	Jurs-RPSA	Spatial	Relative polar surface area
13	S_sCH3	Electrotopological	Sum for a methyl group
14	S_ssCH2	Electrotopological	Sum for a methylene group
15	S_dssC	Electrotopological	Sum for a carbon atom with a double bond and two single bonds (i.e., a carbonyl carbon)
16	S_aasC	Electrotopological	Sum for a carbon atom with a single bond and two aromatic bonds (i.e., a carbon of the pyrrole ring)
17	S_ssNH	Electrotopological	Sum for a nitrogen atom linked to a hydrogen and involved in two additional single bonds (i.e., the NH group of the pyrimidinedione system)
18	S_aaNH	Electrotopological	Sum for a nitrogen atom linked to a hydrogen and involved in two additional aromatic bonds (i.e., the NH group of the pyrrole ring)
19	S_dO	Electrotopological	Sum for an oxygen atom bound through a double bond (i.e., a carbonyl oxygen)
20	S_ssO	Electrotopological	Sum for an oxygen atom bound through two single bonds (i.e., the oxygen of a methoxy group)
21	S_sCl	Electrotopological	Sum for a chlorine atom

[a] Further details on molecular descriptors are available at the QSAR+ theory page of the Accelrys Web site http://www.accelrys.com/doc/life/cerius481/qsar/Output/theory_d_nf.html.

Table 3. Overview of the Eight Best QSAR Models Obtained by Means of the GFA Algorithm on 21 Molecular Descriptors Calculated for Compounds **21**−**40**

no.	QSAR equation and statistical parameters[a]
1	Aff = 21.0309 + 0.715137 HOMO − 1.53546 S_ssCH2 + 0.089448 MR − 0.00095 PMI-mag r^2 = 0.920222, CV r^2 = 0.734, LOF = 0.200777
2	Aff = 30.9349 − 1.42254 S_ssCH2 − 0.00085 PMI-mag + 0.978227 HOMO r^2 = 0.843812, LOF = 0.221106
3	Aff = 14.9317 − 1.28305 S_ssCH2 − 0.001135 PMI-mag + 0.590941 S_dO + 0.88154 HOMO r^2 = 0.881520, LOF = 0.298178
4	Aff = −1.42385 + 0.218582 MR − 0.000713 PMI-mag − 1.41618 S_ssCH2 + 13.7639 Jurs-RPCG r^2 = 0.881415, LOF = 0.298444
5	Aff = 35.7893 − 0.001058 PMI-mag + 1.20452 HOMO − 1.71175 S_ssCH2 + 0.430969 Jurs-RPCS r^2 = 0.877877, LOF = 0.307347
6	Aff = 29.5356 − 0.033243 S_sCl − 1.4278 S_ssCH2 − 0.000758 PMI-mag + 0.880362 HOMO r^2 = 0.870094, LOF = 0.326934
7	Aff = 18.8665 + 1.10796 Jurs-RNCS − 1.43661 S_ssCH2 + 0.093934 MR − 0.000938 PMI-mag + 0.664025 HOMO r^2 = 0.941940, LOF = 0.328768
8	Aff = 30.219 − 0.000863 PMI-mag + 0.938424 HOMO − 1.40417 S_ssCH2 + 0.037602 S_ssO r^2 = 0.869239, LOF = 0.329087

[a] Aff represents log(1/K_i) where K_i is the affinity of compounds toward α_1-ARs, expressed in nM. r^2, CV r^2, and LOF are the correlation coefficient, the cross-validated correlation coefficient, and the lack-of-fit values, respectively. A brief description of molecular descriptors is reported in Table 2.

pended on the electronic descriptor HOMO that should roughly measure the nucleophilicity of a molecule. Thus, molecules able to donate their electrons should be characterized by enhanced affinity. In this context, it is very important to note that compounds **22**−**40** are all characterized by hydrogen bond acceptor systems (one of them, the 4-carbonyl group, has been recognized as a crucial element for interacting with the pharmacophore model) and a piperazine nitrogen atom able to be a positive ionizable group. Moreover, eq 3 showed that affinity was dependent on S_dO (dO represents an oxygen atom bound through a double bond, that is, a carbonyl oxygen), an electrotopological state key encoding information about both the topological environment of that atom and the electronic interactions due to all other atoms in the molecule.[35,36] The second term of the best model was S_ssCH$_2$ (describing a contribution from a methylene group)[35,36] that rationalized the presence of an alkyl spacer. In particular, its negative coefficient accounted for decreased affinity of compounds with a propyl spacer with respect to the corresponding ethyl derivatives (**23** and **24** versus **21** and **22**, **27** and **28** versus **25** and **26**, **37** and **38** versus **35** and **36**). In addition, a molecular refractivity (MR) term, measuring the volume and density of the compounds, was frequently represented in QSAR equations found. Its positive coefficient seemed to show that the binding site for these compounds had a certain tolerance to the bulkiness of the inhibitors, in agreement with the trend of affinity showing that the *o*-methoxyphenylpiperazinyl derivatives were more potent inhibitors with respect to the corresponding *o*-chloro derivatives (with the exception of compound pairs **21** and **22** and compound pairs **30** and **31**, where methoxy derivatives showed slightly lower or comparable activity in comparison to chloro analogues). This finding was also in agreement with the variables S_sCl and S_ssO[35,36] that appeared in eqs 6 and 8, respectively, indicating a negative contribution to the activity from the chloro substituent but a positive contribution from the methoxy group. From a quantita-

Table 4. Calculated (Estimated or Predicted) and Actual Affinity Data for Compounds **21**−**40**

	affinity toward α_1-adrenoreceptor[a]		
compd	actual	calculated[b]	GFA residuals activity[c]
21	8.64	9.06	−0.42
22	9.03	8.79	0.24
23	7.55	7.41	0.14
24	7.22	7.19	0.03
25	9.28	9.11	0.17
26	8.97	8.96	0.01
27	8.91	8.82	0.09
28[d]	7.21	7.22	−0.01
29[e]	<4		
30	9.12	8.91	0.21
31[d]	9.34	9.35	−0.01
32[d]	7.71	8.40	−0.69
33	8.11	8.08	0.03
34	7.93	7.91	0.02
35	8.69	8.67	0.02
36[d]	7.76	8.76	−1.00
37	7.32	7.58	−0.26
38[d]	6.96	6.87	0.09
39	9.11	9.07	0.04
40	8.47	8.80	−0.33
1[d]	9.68	9.26	0.42
2[d]	9.28	8.97	0.31
3[d]	7.89	7.50	0.39

[a] Expressed as $\log(1/K_i)$ where K_i is the affinity of compounds toward α_1-ARs in nM. [b] Estimated (training set) or predicted (test set) affinity values using eq 1 in Table 3. [c] Difference between actual and calculated affinity values. [d] Compounds belonging to the test set. With the exception of **29** (see below), the remaining compounds were included in the training set. [e] Compound not considered in the GFA QSAR analysis.

tive point of view, the positive effect of MR on affinity was counterbalanced by the opposite effect due to the S_ssCH$_2$ variable. Next, the principal moment of inertia (PMI, a spatial descriptor) accounted for the fact that orientation of the molecules and distribution of their chemical groups were important for affinity. Finally, two additional spatial descriptors (relative positive charge surface, RPCS, and relative negative charge surface, RNCS, belonging to the Jurs family of descriptors, calculated by mapping atomic partial charges on solvent-accessible surface areas of each atom) participated in eqs 5 and 7, respectively, to describe affinity on the basis of both shape and electronic information characterizing the molecules.

3. Validation of the QSAR Models. With the aim of validating the QSAR analysis, three different approaches have been chosen. (i) Eight compounds (namely, **1**−**3**,[17] **28**, **31**, **32**, **36**, and **38**) were used to generate a test set to be submitted to affinity prediction through the best QSAR model (model no.1 in Table 3). Results of affinity prediction was summarized in Table 4. In detail, the QSAR equation produces predicted affinity values for compounds **28**, **31**, and **38** (7.22, 9.35, and 6.87, respectively) in very good agreement with experimental data (7.21, 9.34, and 6.96, respectively). On the other hand, poorer predictions were found for **1**−**3**, **32**, and **36** (9.26 vs 9.68, 8.97 vs 9.28, 7.50 vs 7.89, 8.40 vs 7.71, and 8.76 vs 7.76, respectively). (ii) To perform a randomization test, affinity values were repeatedly scrambled to generate 19 new spreadsheets containing both the dependent variable (scrambled affinity) and independent variables (molecular descriptors). The original QSAR model can be considered statistically significant if its statistical parameters are better than those derived from the scrambled sets of data. A summary of the results obtained through the randomization test from 19 trials follows; r from the nonrandom model was 0.959, markedly better than the values obtained from randomized data (mean value of r from random trials was 0.625, with a standard deviation of 0.202). All the scrambled sets produced models with r lower than 0.959 at the 95% confidence level. (iii) A leave-one-out cross-validation encompassing both the optimization of the choice of descriptors and the optimization of regression coefficients was also performed on the best QSAR model. Statistical parameters for the cross-validated model were CV r^2 of 0.835, PRESS of 1.066, and a sum of squares deviation of 6.471.

Conclusions

A new series of 3-arylpiperazinylalkylpyrrolo[3,2-*d*]-pyrimidine-2,4-diones, structurally related to RN5 and characterized by remarkable α_1-AR affinity coupled to high selectivity over 5-HT$_{1A}$, D$_1$, and D$_2$ receptors, has been discovered.

A structure−affinity relationships analysis revealed some structural features that, in this class of compounds, are important to ensure high affinity and selectivity. Replacement of a methoxy group with a chlorine atom in the 2-position of the phenyl ring in the PPz moiety gave compounds (**22**, **31**, **34**, **36**, **40**) with the best 5-HT$_{1A}$/α_1 selectivity ratio. Among them, compounds **34** and **36** are noteworthy for their α_1-AR selectivity over all the other tested receptors. An ethylene alkyl chain connecting the PPz to the PPm moiety seems to be optimum for α_1-AR affinity. The length of this spacer is critical because its elongation by addition of a methylene unit invariably led to a remarkable loss in both α_1-AR affinity and selectivity. With reference to structural modifications on the PPm moiety, most compounds bearing a substituent at the 4- or 2-position of the phenyl ring (**31**, **33**−**36**, **39**, **40**) are endowed with higher selectivity for α_1-ARs with respect to the corresponding unsubstituted analogues **25** and **26**. However, a notable α_1-AR selectivity is also displayed by derivative **22**, which lacks the phenyl ring at the 6-position of the PPm portion. Thus, the pattern of substitutions of the PPm moiety seems to play a significant role in determining α_1-AR selectivity over the other tested receptors.

Moreover, in an effort to correlate α_1-AR affinity of the new compounds with their three-dimensional structure, two different molecular modeling approaches were applied. In the first attempt, analysis of how well such compounds fitted a pharmacophoric model for α_1-AR antagonists allowed us to rationalize affinity data for compounds bearing a hydrogen atom or a phenyl ring or a 2-chlorophenyl moiety at the 6-position of the PPm moiety. In fact, predicted affinities were in good agreement with experimental data. However, the pharmacophoric model was unable to make satisfactory predictions for compounds bearing a 3- or 4-substituted phenyl ring. To get over this limitation, a GFA-based QSAR analysis was performed and several equations were generated. They described affinity as dependent on the length of the alkyl spacer and on the presence of oxygen atoms able to be hydrogen bond acceptors, in agreement

with what was found by means of the pharmacophore model. In addition, QSAR equations correlated affinity with the principal moment of inertia and molar refractivity, two molecular properties that a pharmacophoric-based study is unable to evaluate. Finally, results from the QSAR validation steps suggested the GFA model as a predictive tool to evaluate the α_1-AR affinity of new compounds.

In conclusion, within this new class of α_1-AR ligands, compound **31** emerges over the other described derivatives because of its subnanomolar α_1-AR affinity and high selectivity over the serotoninergic 5-HT_{1A} and dopaminergic D_1 and D_2 receptors. An outstanding α_1-AR selectivity also characterizes the binding profiles of compounds **34** and **36**. These two derivatives, along with **31**, have been selected and an additional study is in progress in order to investigate their activities in functional assays and their affinities for the α_1-AR subtypes.

Experimental Section

Chemistry. Melting points were determined in a Gallenkamp apparatus with an MFB-59 digital thermometer in glass capillary tubes and are uncorrected. Elemental analyses for C, H, N, and S were within ±0.4% of theoretical values and were performed on a Carlo Erba elemental analyzer model 1108 apparatus. ^{1}H NMR spectra were recorded at 200 MHz on a Varian Inova Unity 200 spectrometer in DMSO-d_6 solution. Chemical shifts are given in δ values (ppm), using tetramethylsilane as the internal standard; coupling constants (J) are given in hertz (Hz). Signal multiplicities are characterized as s (singlet), d (doublet), t (triplet), q (quartet), m (multiplet), br (broad signal). All the synthesized compounds were tested for purity on TLC (aluminum sheet coated with silica gel 60 F_{254}, Merck) and visualized by UV (λ = 254 and 366 nm). All chemicals and solvents were reagent grade and were purchased from commercial vendors. Compounds **4**−**8** and **10** were synthesized as previously reported.[21−24]

3-Amino-5-(4-methylphenyl)-1*H*-pyrrole-2-carboxylic Acid Ethyl Ester (9). To a solution of 4-methylbenzoyl acetonitrile (3.90 g, 24.54 mmol) and *p*-toluenesulfonic anhydride (9.60 g, 29.45 mmol) in 50 mL of dry CH_2Cl_2 was added, dropwise, 5.10 mL of Et_3N (36.81 mmol). After 16 h of stirring at 22 °C, the reaction mixture was diluted with H_2O and extracted with CH_2Cl_2 (4 × 50 mL). The combined organic layers were dried over Na_2SO_4, filtered, and concentrated in vacuo to give an orange solid. The obtained crude material was recrystallized from EtOH to give 4.80 g of 2-cyano-1-(4-methylphenyl)vinyl 4-methylbenzenesulfonate as a white solid (62%): mp 125−127 °C; ^{1}H NMR (DMSO-d_6) δ 2.33 (s, 3 H, CH_3), 2.42 (s, 3 H, CH_3), 6.55 (s, 1 H, CH), 7.19−7.28 (m, 2 H, aromatic), 7.44−7.51 (m, 4 H, aromatic), 7.78−7.89 (m, 2 H, aromatic). Anal. ($C_{17}H_{15}NO_3S$) C, H, N, S.

To a solution of sodium ethoxide freshly prepared from Na (1.03 g, 44.64 mmol) and absolute EtOH (28 mL) under nitrogen atmosphere was slowly added a suspension of 2-cyano-1-(4-methylphenyl)vinyl 4-methylbenzenesulfonate (4.66 g, 14.88 mmol) and diethyl aminomalonate hydrochloride (3.15 g, 14.88 mmol) in 60 mL of EtOH and 6 mL of THF. After the addition was completed, the reaction mixture was stirred at 22 °C for 2 h and concentrated under reduced pressure to give an orange solid. The obtained crude material was diluted with 50 mL of water and extracted with EtOAc (3 × 50 mL). The combined organic layers were dried over Na_2SO_4 and concentrated under reduced pressure. The obtained orange solid was recrystallized from EtOH to give 1.27 g of a white powder (35%): mp 167−169 °C; ^{1}H NMR (DMSO-d_6) δ 1.30 (t, J = 7.0 Hz, 3 H, OCH_2CH_3), 2.30 (s, 3 H, CH_3), 4.23 (q, J = 7.0 Hz, 2 H, OCH_2CH_3), 5.11 (br s, 2 H, NH_2 which exchanges with D_2O), 6.01 (d, ^4J = 2.8 Hz, 1 H, pyrrole), 7.21−7.28 (m, 2 H, aromatic), 7.74−7.78 (m, 2 H, aromatic), 10.78 (br s, 1 H, NH which exchanges with D_2O). Anal. ($C_{14}H_{16}N_2O_2$) C, H, N.

General Procedure for the Preparation of *N*-Chloroalkyl-*N*′-[3-(2-ethoxycarbonyl-5-substituted)-1*H*-pyrrolyl]-ureas (11−20). A suspension of the appropriate 3-amino-5-substituted-1*H*-pyrrole-2-carboxylic acid ethyl ester (20 mmol) and the appropriate chloroalkyl isocyanate (30 mmol) in 40 mL of toluene was stirred for 16 h at 22 °C. The reaction mixture was then filtered, and the obtained solid was washed several times with EtOH to give the desired product as a pure solid.

By use of this procedure, the subsequent compounds were obtained.

***N*-(2-Chloroethyl)-*N*′-[3-(2-ethoxycarbonyl)-1*H*-pyrrolyl]urea (11).** The title compound was obtained as a white powder (90%): mp 177−179 °C; ^{1}H NMR (DMSO-d_6) δ 1.30 (t, J = 7.0 Hz, 3 H, OCH_2CH_3), 3.40−3.43 (m, 2 H, $NHCH_2$), 3.63 (t, J = 6.0 Hz, 2 H, CH_2Cl), 4.27 (q, J = 7.0 Hz, 2 H, OCH_2CH_3), 6.65−6.68 (m, 1 H, pyrrole), 6.80−6.83 (m, 1 H, pyrrole), 7.61 (br t, J = 5.4 Hz, 1 H, $NHCONHCH_2$ which exchanges with D_2O), 8.43 (br s, 1 H, $NHCONHCH_2$ which exchanges with D_2O), 11.24 (br s, 1 H, NH which exchanges with D_2O). Anal. ($C_{10}H_{14}ClN_3O_3$) C, H, N.

***N*-(3-Chloropropyl)-*N*′-[3-(2-ethoxycarbonyl)-1*H*-pyrrolyl]urea (12).** The title compound was obtained as a white powder (80%): mp 78−80 °C; ^{1}H NMR (DMSO-d_6) δ 1.29 (t, J = 7.0 Hz, 3 H, OCH_2CH_3), 1.83−1.89 (m, 2 H, $CH_2CH_2CH_2$), 3.13−3.25 (m, 2 H, $NHCH_2$), 3.67 (t, J = 6.4 Hz, 2 H, CH_2Cl), 4.26 (q, J = 7.0 Hz, 2 H, OCH_2CH_3), 6.65−6.68 (m, 1 H, pyrrole), 6.79−6.82 (m, 1 H, pyrrole), 7.33 (br t, J = 5.4 Hz, 1 H, $NHCONHCH_2$ which exchanges with D_2O), 8.34 (br s, 1 H, $NHCONHCH_2$ which exchanges with D_2O), 11.20 (br s, 1 H, NH which exchanges with D_2O). Anal. ($C_{11}H_{16}ClN_3O_3$) C, H, N.

***N*-(2-Chloroethyl)-*N*′-[3-(2-ethoxycarbonyl-5-phenyl)-1*H*-pyrrolyl]urea (13).** The title compound was obtained as a white powder (79%): mp 227−228 °C; ^{1}H NMR (DMSO-d_6) δ 1.34 (t, J = 7.0 Hz, 3 H, OCH_2CH_3), 3.35−3.43 (m, 2 H, $NHCH_2$), 3.66 (t, J = 6.0 Hz, 2 H, CH_2Cl), 4.32 (q, J = 7.0 Hz, 2 H, OCH_2CH_3), 7.12 (d, ^4J = 2.8 Hz, 1 H, pyrrole), 7.29−7.44 (m, 3 H, aromatic), 7.69 (br t, J = 5.6 Hz, 1 H, $NHCONHCH_2$ which exchanges with D_2O), 7.77−7.81 (m, 2 H, aromatic), 8.52 (br s, 1 H, $NHCONHCH_2$ which exchanges with D_2O), 11.42 (br s, 1 H, NH which exchanges with D_2O). Anal. ($C_{16}H_{18}ClN_3O_3$) C, H, N.

***N*-(3-Chloropropyl)-*N*′-[3-(2-ethoxycarbonyl-5-phenyl)-1*H*-pyrrolyl]urea (14).** The title compound was obtained as a white powder (76%): mp 190−191 °C; ^{1}H NMR (DMSO-d_6) δ 1.34 (t, J = 7.0 Hz, 3 H, OCH_2CH_3), 1.86−1.93 (m, 2 H, $CH_2CH_2CH_2$), 3.17−3.26 (m, 2 H, $NHCH_2$), 3.70 (t, J = 6.4 Hz, 2 H, CH_2Cl), 4.32 (q, J = 7.0 Hz, 2 H, OCH_2CH_3), 7.13 (d, ^4J = 2.8 Hz, 1 H, pyrrole), 7.26−7.44 (m, 3 H + 1 H, aromatic + $NHCONHCH_2$ which exchanges with D_2O), 7.77−7.81 (m, 2 H, aromatic), 8.44 (br s, 1 H, $NHCONHCH_2$ which exchanges with D_2O), 11.39 (br s, 1 H, NH which exchanges with D_2O). Anal. ($C_{17}H_{20}ClN_3O_3$) C, H, N.

***N*-(2-Chloroethyl)-*N*′-[3-[2-ethoxycarbonyl-5-(2-chlorophenyl)-1*H*-pyrrolyl]]urea (15).** The title compound was obtained as a white powder (85%): mp 156−158 °C; ^{1}H NMR (DMSO-d_6) δ 1.32 (t, J = 7.0 Hz, 3 H, OCH_2CH_3), 3.38−3.44 (m, 2 H, $NHCH_2$), 3.65 (t, J = 6.0 Hz, 2 H, CH_2Cl), 4.30 (q, J = 7.0 Hz, 2 H, OCH_2CH_3), 7.08 (d, ^4J = 2.8 Hz, 1 H, pyrrole), 7.33−7.44 (m, 2 H, aromatic), 7.52−7.62 (m, 2 H, aromatic), 7.69 (br t, J = 5.6 Hz, 1 H, $NHCONHCH_2$ which exchanges with D_2O), 8.51 (br s, 1 H, $NHCONHCH_2$ which exchanges with D_2O), 11.48 (br s, 1 H, NH which exchanges with D_2O). Anal. ($C_{16}H_{17}Cl_2N_3O_3$) C, H, N.

***N*-(2-Chloroethyl)-*N*′-[3-[2-ethoxycarbonyl-5-(3-chlorophenyl)-1*H*-pyrrolyl]]urea (16).** The title compound was obtained as a white powder (82%): mp 170−172 °C; ^{1}H NMR (DMSO-d_6) δ 1.35 (t, J = 7.0 Hz, 3 H, OCH_2CH_3), 3.40−3.46 (m, 2 H, $NHCH_2$), 3.66 (t, J = 6.0 Hz, 2 H, CH_2Cl), 4.33 (q, J = 7.0 Hz, 2 H, OCH_2CH_3), 7.18 (d, ^4J = 2.8 Hz, 1 H, pyrrole), 7.31−7.47 (m, 2 H, aromatic), 7.67−7.75 (m, 1 H + 1 H, aromatic + $NHCONHCH_2$ which exchanges with D_2O), 7.97 (m, 1 H, aromatic), 8.53 (br s, 1 H, $NHCONHCH_2$ which

exchanges with D_2O), 11.56 (br s, 1 H, NH which exchanges with D_2O). Anal. ($C_{16}H_{17}Cl_2N_3O_3$) C, H, N.

***N*-(2-Chloroethyl)-*N′*-[3-[2-ethoxycarbonyl-5-(4-chlorophenyl)-1*H*-pyrrolyl]]urea (17).** The title compound was obtained as a white powder (70%): mp 248−249 °C; ^{1}H NMR (DMSO-d_6) δ 1.34 (t, J = 7.0 Hz, 3 H, OCH_2CH_3), 3.36−3.45 (m, 2 H, $NHCH_2$), 3.66 (t, J = 5.8 Hz, 2 H, CH_2Cl), 4.32 (q, J = 7.0 Hz, 2 H, OCH_2CH_3), 7.14 (d, ^4J = 2.8 Hz, 1 H, pyrrole), 7.43−7.48 (m, 2 H, aromatic), 7.69 (br t, J = 5.4 Hz, 1 H, $NHCONHCH_2$ which exchanges with D_2O), 7.80−7.84 (m, 2 H, aromatic), 8.52 (br s, 1 H, $NHCONHCH_2$ which exchanges with D_2O), 11.50 (br s, 1 H, NH which exchanges with D_2O). Anal. ($C_{16}H_{17}Cl_2N_3O_3$) C, H, N.

***N*-(2-Chloroethyl)-*N′*-[3-[2-ethoxycarbonyl-5-(4-methylphenyl)-1*H*-pyrrolyl]]-urea (18).** The title compound was obtained as a white powder (89%): mp 180−182 °C; ^{1}H NMR (DMSO-d_6) δ 1.34 (t, J = 7.0 Hz, 3 H, OCH_2CH_3), 2.31 (s, 3 H, CH_3), 3.40−3.45 (m, 2 H, $NHCH_2$), 3.66 (t, J = 6.0 Hz, 2 H, CH_2Cl), 4.31 (q, J = 7.0 Hz, 2 H, OCH_2CH_3), 7.08 (d, ^4J = 2.8 Hz, 1 H, pyrrole), 7.19−7.23 (m, 2 H, aromatic), 7.67−7.71 (m, 2 H + 1 H, aromatic + $NHCONHCH_2$ which exchanges with D_2O), 8.52 (br s, 1 H, $NHCONHCH_2$ which exchanges with D_2O), 11.37 (br s, 1 H, NH which exchanges with D_2O). Anal. ($C_{17}H_{20}ClN_3O_3$) C, H, N.

***N*-(3-Chloropropyl)-*N′*-[3-[2-ethoxycarbonyl-5-(4-methylphenyl)-1*H*-pyrrolyl]]urea (19).** The title compound was obtained as a white powder (61%): mp 212−214 °C; ^{1}H NMR (DMSO-d_6) δ 1.33 (t, J = 7.0 Hz, 3 H, OCH_2CH_3), 1.85−1.92 (m, 2 H, $CH_2CH_2CH_2$), 2.31 (s, 3 H, CH_3), 3.16−3.25 (m, 2 H, $NHCH_2$), 3.69 (t, J = 6.4 Hz, 2 H, CH_2Cl), 4.30 (q, J = 7.0 Hz, 2 H, OCH_2CH_3), 7.07 (d, ^4J = 2.6 Hz, 1 H, pyrrole), 7.18−7.22 (m, 2 H, aromatic), 7.40 (br t, J = 5.6 Hz, 1 H, $NHCONHCH_2$ which exchanges with D_2O), 7.66−7.70 (m, 2 H, aromatic), 8.44 (br s, 1 H, $NHCONHCH_2$ which exchanges with D_2O), 11.31 (br s, 1 H, NH which exchanges with D_2O). Anal. ($C_{18}H_{22}ClN_3O_3$) C, H, N.

***N*-(2-Chloroethyl)-*N′*-{3-[2-ethoxycarbonyl-5-(4-methoxyphenyl)-1*H*-pyrrolyl]}urea (20).** The title compound was obtained as a white powder (80%): mp 178−180 °C; ^{1}H NMR (DMSO-d_6) δ 1.33 (t, J = 7.0 Hz, 3 H, OCH_2CH_3), 3.40−3.45 (m, 2 H, $NHCH_2$), 3.66 (t, J = 6.0 Hz, 2 H, CH_2Cl), 3.78 (s, 3 H, OCH_3), 4.31 (q, J = 7.0 Hz, 2 H, OCH_2CH_3), 6.94−7.03 (m, 1 H + 2 H, pyrrole + aromatic), 7.65−7.75 (m, 2 H + 1 H, aromatic + $NHCONHCH_2$ which exchanges with D_2O), 8.52 (br s, 1 H, $NHCONHCH_2$ which exchanges with D_2O), 11.27 (br s, 1 H, NH which exchanges with D_2O). Anal. ($C_{17}H_{20}ClN_3O_4$) C, H, N.

Method A: General Procedure for the Preparation of 3-[[4-(Substituted phenyl)piperazin-1-yl]alkyl]-6-substituted-1,5-dihydropyrrolo[3,2-*d*]pyrimidine-2,4-diones (21−24, 27, 28, 31, 37−40). A suspension of the appropriate (ω-chloroalkyl)urea (0.50 mmol), the appropriate 1-(substituted phenyl)piperazine hydrochloride (0.75 mmol), $NaHCO_3$ (2.0 mmol), and a catalytic amount of NaI in 2 mL of THF was refluxed for 4 days. After this period the obtained mixture was concentrated and the residue was diluted with water (50 mL) and extracted with CH_2Cl_2 (3 × 50 mL). The combined organic layers were dried over Na_2SO_4, filtered, and evaporated. The obtained crude material was refluxed in methanolic KOH (1 N, 1.5 mL) for 2 h. The reaction mixture was then allowed to cool at 22 °C, acidified (pH 4) with glacial AcOH, and neutralized with saturated $NaHCO_3$. A brown precipitate was isolated, washed with water and EtOH, and finally recrystallized from DMF/water (2:1) to afford the desired products as solids.

3-[2-[4-(2-Methoxyphenyl)piperazin-1-yl]ethyl]-1,5-dihydropyrrolo[3,2-*d*]pyrimidine-2,4-dione (21). The title compound was isolated as a white powder (79%): mp 308−309 °C; ^{1}H NMR (DMSO-d_6) δ 2.35−2.79 (m, 4 H + 2 H, NCH_2 + $CONCH_2CH_2N$), 2.85−3.09 (m, 4 H, NCH_2), 3.74 (s, 3 H, CH_3), 4.02 (t, J = 6.6 Hz, 2 H, $CONCH_2CH_2N$), 5.85 (d, J = 2.6 Hz, 1 H, pyrrole), 6.79−6.97 (m, 4 H, aromatic), 7.28 (d, 1 H, J = 2.6 Hz, pyrrole), 11.09 (br s, 1 H, NH which exchanges with D_2O), 11.91 (br s, 1 H, NH which exchanges with D_2O). Anal. ($C_{19}H_{23}N_5O_3$) C, H, N.

3-[2-[4-(2-Chlorophenyl)piperazin-1-yl]ethyl]-1,5-dihydropyrrolo[3,2-*d*]pyrimidine-2,4-dione (22). The title compound was isolated as a white powder (85%): mp 285−287 °C; ^{1}H NMR (DMSO-d_6) δ 2.49−2.77 (m, 4 H + 2 H, NCH_2 + $CONCH_2CH_2N$), 2.85−3.09 (m, 4 H, NCH_2), 4.01 (t, J = 6.6 Hz, 2 H, $CONCH_2CH_2N$), 5.85 (d, J = 2.6 Hz, 1 H, pyrrole), 6.98−7.42 (m, 4 H + 1 H, aromatic + pyrrole), 11.11 (br s, 1 H, NH which exchanges with D_2O), 11.92 (br s, 1 H, NH which exchanges with D_2O). Anal. ($C_{18}H_{20}ClN_5O_2$) C, H, N.

3-[3-[4-(2-Methoxyphenyl)piperazin-1-yl]propyl]-1,5-dihydropyrrolo[3,2-*d*]pyrimidine-2,4-dione (23). The title compound was isolated as a white powder (70%): mp 225−227 °C; ^{1}H NMR (DMSO-d_6) δ 1.63−1.77 (m, 2 H, $CONCH_2CH_2CH_2N$), 2.34−2.59 (m, 4 H + 2 H, NCH_2 + $CONCH_2CH_2CH_2N$), 2.86−2.99 (m, 4 H, NCH_2), 3.76 (s, 3 H, CH_3), 3.91 (t, J = 6.6 Hz, 2 H, $CONCH_2CH_2CH_2N$), 5.84 (d, J = 2.6 Hz, 1 H, pyrrole), 6.83−6.94 (m, 4 H, aromatic), 7.15 (d, 1 H, J = 2.6 Hz, pyrrole), 11.12 (br s, 1 H, NH which exchanges with D_2O), 11.95 (br s, 1 H, NH which exchanges with D_2O). Anal. ($C_{20}H_{25}N_5O_3$) C, H, N.

3-[3-[4-(2-Chlorophenyl)piperazin-1-yl]propyl]-1,5-dihydropyrrolo[3,2-*d*]pyrimidine-2,4-dione (24). The title compound was isolated as a white powder (89%): mp 223−225 °C; ^{1}H NMR (DMSO-d_6) δ 1.71−1.77 (m, 2 H, $CH_2CH_2CH_2$), 2.34−2.60 (m, 4 H + 2 H, NCH_2 + $CONCH_2CH_2CH_2N$), 2.82−2.97 (m, 4 H, NCH_2), 3.92 (t, J = 6.6 Hz, 2 H, $CONCH_2CH_2CH_2N$), 5.86 (d, J = 2.6 Hz, 1 H, pyrrole), 6.80−7.41 (m, 4 H + 1 H, aromatic + pyrrole), 11.09 (br s, 1 H, NH which exchanges with D_2O), 11.88 (br s, 1 H, NH which exchanges with D_2O). Anal. ($C_{19}H_{22}ClN_5O_2$) C, H, N.

3-[3-[4-(2-Methoxyphenyl)piperazin-1-yl]propyl]-6-phenyl-1,5-dihydropyrrolo[3,2-*d*]pyrimidine-2,4-dione (27). The title compound was isolated as a white powder (69%): mp 324−325 °C; ^{1}H NMR (DMSO-d_6) δ 1.65−1.79 (m, 2 H, $CONCH_2CH_2CH_2N$), 2.32−2.58 (m, 4 H + 2 H, NCH_2 + $CONCH_2CH_2CH_2N$), 2.82−2.94 (m, 4 H, NCH_2), 3.76 (s, 3 H, CH_3), 3.95 (t, J = 6.6 Hz, 2 H, $CONCH_2CH_2CH_2N$), 6.31 (s, 1 H, pyrrole), 6.80−6.93 (m, 4 H, aromatic), 7.29−7.46 (m, 3 H, aromatic), 7.86−7.90 (m, 2 H, aromatic), 11.15 (br s, 1 H, NH which exchanges with D_2O), 12.24 (br s, 1 H, NH which exchanges with D_2O). Anal. ($C_{26}H_{29}N_5O_3$) C, H, N.

3-[3-[4-(2-Chlorophenyl)piperazin-1-yl]propyl]-6-phenyl-1,5-dihydropyrrolo[3,2-*d*]pyrimidine-2,4-dione (28). The title compound was isolated as a white powder (54%): mp 278−279 °C; ^{1}H NMR (DMSO-d_6) δ 1.66−1.80 (m, 2 H, $CONCH_2CH_2CH_2N$), 2.34−2.61 (m, 4 H + 2 H, NCH_2 + $CONCH_2CH_2CH_2N$), 2.81−2.95 (m, 4 H, NCH_2), 3.96 (t, J = 6.6 Hz, 2 H, $CONCH_2CH_2CH_2N$), 6.29 (s, 1 H, pyrrole), 6.31−7.46 (m, 7 H, aromatic), 7.86−7.89 (m, 2 H, aromatic), 11.16 (br s, 1 H, NH which exchanges with D_2O), 12.20 (br s, 1 H, NH which exchanges with D_2O). Anal. ($C_{25}H_{26}ClN_5O_2$) C, H, N.

3-[2-[4-(2-Chlorophenyl)piperazin-1-yl]ethyl]-6-(2-chlorophenyl)-1,5-dihydropyrrolo[3,2-*d*]pyrimidine-2,4-dione (31). The title compound was isolated as a light-pink powder (51%): mp 280−281 °C; ^{1}H NMR (DMSO-d_6) δ 2.44−2.82 (m, 4 H + 2 H, NCH_2 + $CONCH_2CH_2N$), 2.87−3.16 (m, 4 H, NCH_2), 4.07 (t, J = 6.6 Hz, 2 H, $CONCH_2CH_2N$), 6.25 (s, 1 H, pyrrole), 6.99−7.69 (m, 8 H, aromatic), 11.17 (br s, 1 H, NH which exchanges with D_2O), 12.25 (br s, 1 H, NH which exchanges with D_2O). Anal. ($C_{24}H_{23}Cl_2N_5O_2$) C, H, N.

3-[3-[4-(2-Methoxyphenyl)piperazin-1-yl]propyl]-6-(4-methylphenyl)-1,5-dihydropyrrolo[3,2-*d*]pyrimidine-2,4-dione (37). The title compound was isolated as a white powder (50%): mp 272−273 °C; ^{1}H NMR (DMSO-d_6) δ 1.65−1.91 (m, 2 H, $CONCH_2CH_2CH_2N$), 2.28−2.59 (m, 4 H + 2 H + 3 H, NCH_2 + $CONCH_2CH_2CH_2N$, CH_3), 2.83−2.92 (m, 4 H, NCH_2), 3.75 (s, 3 H, OCH_3), 3.94 (t, J = 6.6 Hz, 2 H, $CONCH_2CH_2CH_2N$), 6.24 (s, 1 H, pyrrole), 6.77−6.90 (m, 4 H, aromatic), 7.20−7.24 (m, 2 H, aromatic), 7.73−7.77 (m, 2 H, aromatic),

11.13 (br s, 1 H, NH which exchanges with D_2O), 12.14 (br s, 1 H, NH which exchanges with D_2O). Anal. ($C_{27}H_{31}N_5O_3$) C, H, N.

3-[3-[4-(2-Chlorophenyl)piperazin-1-yl]propyl]-6-(4-methylphenyl)-1,5-dihydropyrrolo[3,2-*d*]pyrimidine-2,4-dione (38). The title compound was isolated as a white powder (49%): mp 294−296 °C; ^{1}H NMR (DMSO-d_6) δ 1.68−1.84 (m, 2 H, CONCH$_2$C*H*$_2$CH$_2$N), 2.30−2.56 (m, 4 H + 2 H + 3 H, NCH$_2$ + CONCH$_2$CH$_2$C*H*$_2$N, CH$_3$), 2.84−2.95 (m, 4 H, NCH$_2$), 3.94 (t, J = 6.6 Hz, 2 H, CONC*H*$_2$CH$_2$CH$_2$N), 6.25 (s, 1 H, pyrrole), 6.97−7.08 (m, 2 H, aromatic), 7.17−7.25 (m, 3 H, aromatic), 7.36−7.40 (m, 1 H, aromatic), 7.74−7.78 (m, 2 H, aromatic), 11.14 (br s, 1 H, NH which exchanges with D_2O), 12.15 (br s, 1 H, NH which exchanges with D_2O). Anal. ($C_{26}H_{28}ClN_5O_2$) C, H, N.

3-[2-[4-(2-Methoxyphenyl)piperazin-1-yl]ethyl]-6-(4-methoxyphenyl)-1,5-dihydropyrrolo[3,2-*d*]pyrimidine-2,4-dione (39). The title compound was isolated as a white powder (59%): mp 310−312 °C; ^{1}H NMR (DMSO-d_6) δ 2.43−2.75 (m, 4 H + 2 H, NCH$_2$ + CONCH$_2$C*H*$_2$N), 2.85−3.04 (m, 4 H, NCH$_2$), 3.76 (s, 3 H, CH$_3$), 3.79 (s, 3 H, CH$_3$), 4.03 (t, J = 6.6 Hz, 2 H, CONC*H*$_2$CH$_2$N), 6.20 (s, 1 H, pyrrole), 6.86−7.00 (m, 6 H, aromatic), 7.80−7.84 (m, 2 H, aromatic), 11.15 (br s, 1 H, NH which exchanges with D_2O), 12.07 (br s, 1 H, NH which exchanges with D_2O). Anal. ($C_{26}H_{29}N_5O_4$) C, H, N.

3-[2-[4-(2-Chlorophenyl)piperazin-1-yl]ethyl]-6-(4-methoxyphenyl)-1,5-dihydropyrrolo[3,2-*d*]pyrimidine-2,4-dione (40). The title compound was isolated as a white powder (65%): mp 315−317 °C; ^{1}H NMR (DMSO-d_6) δ 2.44−2.78 (m, 4 H + 2 H, NCH$_2$ + CONCH$_2$C*H*$_2$N), 2.85−3.04 (m, 4 H, NCH$_2$), 3.79 (s, 3 H, CH$_3$), 4.04 (t, J = 6.6 Hz, 2 H, CONC*H*$_2$-CH$_2$N), 6.21 (s, 1 H, pyrrole), 6.86−7.00 (m, 6 H, aromatic), 7.80−7.84 (m, 2 H, aromatic), 11.15 (br s, 1 H, NH which exchanges with D_2O), 12.07 (br s, 1 H, NH which exchanges with D_2O). Anal. ($C_{25}H_{26}ClN_5O_3$) C, H, N.

Method B: General Procedure for the Preparation of 3-[2-[4-(Substituted phenyl)piperazin-1-yl]ethyl]-6-aryl-1,5-dihydropyrrolo[3,2-*d*]pyrimidine-2,4-diones (25, 26, 29, 30, 32−36). A mixture of the appropriate (2-chloroethyl)-urea (2.0 mmol) and the appropriate 1-(substituted phenyl)-piperazine (10 mmol) was heated in an oil bath for 2 h at 140 °C. After cooling, the reaction mixture was treated with 15 mL of warm EtOH and the precipitate was filtered off, washed with EtOH and successively with water, and dried. Recrystallization from DMF/water (2:1) gave the desired products as solids.

3-[2-[4-(2-Methoxyphenyl)piperazin-1-yl]ethyl]-6-phenyl-1,5-dihydropyrrolo[3,2-*d*]pyrimidine-2,4-dione (25). The title compound was isolated as a white powder (50%): mp 328−329 °C; ^{1}H NMR (DMSO-d_6) δ 2.40−2.79 (m, 4 H + 2 H, NCH$_2$ + CONCH$_2$C*H*$_2$N), 2.82−3.10 (m, 4 H, NCH$_2$), 3.77 (s, 3 H, CH$_3$), 4.04 (t, J = 6.6 Hz, 2 H, CONC*H*$_2$CH$_2$N), 6.32 (s, 1 H, pyrrole), 6.81−6.95 (m, 4 H, aromatic), 7.35−7.48 (m, 3 H, aromatic), 7.80−7.98 (m, 2 H, aromatic), 11.19 (br s, 1 H, NH which exchanges with D_2O), 12.24 (br s, 1 H, NH which exchanges with D_2O). Anal. ($C_{25}H_{27}N_5O_3$) C, H, N.

3-[2-[4-(2-Chlorophenyl)piperazin-1-yl]ethyl]-6-phenyl-1,5-dihydropyrrolo[3,2-*d*]pyrimidine-2,4-dione (26). The title compound was isolated as a white powder (59%): mp 331−332 °C; ^{1}H NMR (DMSO-d_6) δ 2.56−2.65 (m, 4 H + 2 H, NCH$_2$ + CONCH$_2$C*H*$_2$N), 2.89−3.01 (m, 4 H, NCH$_2$), 4.05 (t, J = 6.6 Hz, 2 H, CONC*H*$_2$CH$_2$N), 6.32 (s, 1 H, pyrrole), 7.03−7.15 (m, 2 H, aromatic), 7.24−7.46 (m, 5 H, aromatic), 7.86−7.90 (m, 2 H, aromatic), 11.17 (br s, 1 H, NH which exchanges with D_2O), 12.23 (br s, 1 H, NH which exchanges with D_2O). Anal. ($C_{24}H_{24}ClN_5O_2$) C, H, N.

3-[2-[4-(4-Methoxyphenyl)piperazin-1-yl]ethyl]-6-phenyl-1,5-dihydropyrrolo[3,2-*d*]pyrimidine-2,4-dione (29). The title compound was isolated as a white powder (50%): mp 371−372 °C; ^{1}H NMR (DMSO-d_6) δ 2.45−2.74 (m, 4 H + 2 H, NCH$_2$ + CONCH$_2$C*H*$_2$N), 2.82−3.10 (m, 4 H, NCH$_2$), 3.67 (s, 3 H, CH$_3$), 4.04 (t, J = 6.6 Hz, 2 H, CONC*H*$_2$CH$_2$N), 6.31 (s, 1 H, pyrrole), 6.82−6.90 (m, 4 H, aromatic), 7.32−7.42 (m, 3 H, aromatic), 7.85−7.89 (m, 2 H, aromatic), 11.19 (br s, 1 H, NH which exchanges with D_2O), 12.23 (br s, 1 H, NH which exchanges with D_2O). Anal. ($C_{25}H_{27}N_5O_3$) C, H, N.

6-(2-Chlorophenyl)-3-[2-[4-(2-methoxyphenyl)piperazin-1-yl]ethyl]-1,5-dihydropyrrolo[3,2-*d*]pyrimidine-2,4-dione (30). The title compound was isolated as a white powder (43%): mp 291−292 °C; ^{1}H NMR (DMSO-d_6) δ 2.45−2.76 (m, 4 H + 2 H, NCH$_2$ + CONCH$_2$C*H*$_2$N), 2.85−3.10 (m, 4 H, NCH$_2$), 3.77 (s, 3 H, CH$_3$), 4.05 (t, J = 6.6 Hz, 2 H, CONC*H*$_2$-CH$_2$N), 6.25 (s, 1 H, pyrrole), 6.82−7.00 (m, 4 H, aromatic), 7.39−7.44 (m, 2 H, aromatic), 7.56−7.69 (m, 2 H, aromatic), 11.17 (br s, 1 H, NH which exchanges with D_2O), 12.23 (br s, 1 H, NH which exchanges with D_2O). Anal. ($C_{25}H_{26}ClN_5O_3$) C, H, N.

6-(3-Chlorophenyl)-3-[2-[4-(2-methoxyphenyl)piperazin-1-yl]ethyl]-1,5-dihydropyrrolo[3,2-*d*]pyrimidine-2,4-dione (32). The title compound was isolated as a white powder (39%): mp 297−298 °C; ^{1}H NMR (DMSO-d_6) δ 2.45−2.76 (m, 4 H + 2 H, NCH$_2$ + CONCH$_2$C*H*$_2$N), 2.85−3.00 (m, 4 H, NCH$_2$), 3.77 (s, 3 H, CH$_3$), 4.04 (t, J = 6.6 Hz, 2 H, CONC*H*$_2$-CH$_2$N), 6.43 (s, 1 H, pyrrole), 6.86−6.91 (m, 4 H, aromatic), 7.36−7.49 (m, 2 H, aromatic), 7.83−7.87 (m, 1 H, aromatic), 8.30−8.39 (m, 1 H, aromatic), 11.26 (br s, 1 H, NH which exchanges with D_2O), 12.35 (br s, 1 H, NH which exchanges with D_2O). Anal. ($C_{25}H_{26}ClN_5O_3$) C, H, N.

6-(4-Chlorophenyl)-3-[2-[4-(2-methoxyphenyl)piperazin-1-yl]ethyl]-1,5-dihydropyrrolo[3,2-*d*]pyrimidine-2,4-dione (33). The title compound was isolated as a white powder (55%): mp 334−335 °C; ^{1}H NMR (DMSO-d_6) δ 2.40−2.65 (m, 4 H + 2 H, NCH$_2$ + CONCH$_2$C*H*$_2$N), 2.80−3.00 (m, 4 H, NCH$_2$), 3.76 (s, 3 H, CH$_3$), 4.03 (t, J = 6.6 Hz, 2 H, CONC*H*$_2$-CH$_2$N), 6.35 (s, 1 H, pyrrole), 6.85−6.91 (m, 4 H, aromatic), 7.45−7.50 (m, 2 H, aromatic), 7.88−7.93 (m, 2 H, aromatic), 11.21 (br s, 1 H, NH which exchanges with D_2O), 12.30 (br s, 1 H, NH which exchanges with D_2O). Anal. ($C_{25}H_{26}ClN_5O_3$) C, H, N.

3-[2-[4-(2-Chlorophenyl)piperazin-1-yl]ethyl]-6-(4-chlorophenyl)-1,5-dihydropyrrolo[3,2-*d*]pyrimidine-2,4-dione (34). The title compound was isolated as a white powder (51%): mp 337−338 °C; ^{1}H NMR (DMSO-d_6) δ 2.42−2.75 (m, 4 H + 2 H, NCH$_2$ + CONCH$_2$C*H*$_2$N), 2.90−3.11 (m, 4 H, NCH$_2$), 4.04 (t, J = 6.6 Hz, 2 H, CONC*H*$_2$CH$_2$N), 6.36 (s, 1 H, pyrrole), 6.99−7.15 (m, 4 H, aromatic), 7.25−7.50 (m, 2 H, aromatic), 7.89−7.94 (m, 2 H, aromatic), 11.23 (br s, 1 H, NH which exchanges with D_2O), 12.32 (br s, 1 H, NH which exchanges with D_2O). Anal. ($C_{24}H_{23}Cl_2N_5O_2$) C, H, N.

3-[2-[4-(2-Methoxyphenyl)piperazin-1-yl]ethyl]-6-(4-methylphenyl)-1,5-dihydropyrrolo[3,2-*d*]pyrimidine-2,4-dione (35). The title compound was isolated as a white powder (45%): mp 349−350 °C; ^{1}H NMR (DMSO-d_6) δ 2.32 (s, 3 H, CH$_3$), 2.45−2.66 (m, 4 H + 2 H, NCH$_2$ + CONCH$_2$C*H*$_2$N), 2.85−3.04 (m, 4 H, NCH$_2$), 3.77 (s, 3 H, OCH$_3$), 4.03 (t, J = 6.6 Hz, 2 H, CONC*H*$_2$CH$_2$N), 6.26 (s, 1 H, pyrrole), 6.81−6.95 (m, 4 H, aromatic), 7.18−7.25 (m, 2 H, aromatic), 7.71−7.88 (m, 2 H, aromatic), 11.17 (br s, 1 H, NH which exchanges with D_2O), 12.16 (br s, 1 H, NH which exchanges with D_2O). Anal. ($C_{26}H_{29}N_5O_3$) C, H, N.

3-[2-[4-(2-Chlorophenyl)piperazin-1-yl]ethyl]-6-(4-methylphenyl)-1,5-dihydropyrrolo[3,2-*d*]pyrimidine-2,4-dione (36). The title compound was isolated as a white powder (48%): mp 337−338 °C; ^{1}H NMR (DMSO-d_6) δ 2.32 (s, 3 H, CH$_3$), 2.41−2.75 (m, 4 H + 2 H, NCH$_2$ + CONCH$_2$C*H*$_2$N), 2.86−3.09 (m, 4 H, NCH$_2$), 4.04 (t, J = 6.6 Hz, 2 H, CONC*H*$_2$-CH$_2$N), 6.26 (s, 1 H, pyrrole), 6.94−7.49 (m, 6 H, aromatic), 7.76−7.91 (m, 2 H, aromatic), 11.18 (br s, 1 H, NH which exchanges with D_2O), 12.15 (br s, 1 H, NH which exchanges with D_2O). Anal. ($C_{25}H_{26}ClN_5O_2$) C, H, N.

Pharmacology. Binding Assays. Male CRL:CD(SD)BR-COBS rats weighing about 150 g were killed by decapitation,[37] and their brains were rapidly dissected (hippocampus for 5-HT$_{1A}$; striatum for D_1 and D_2; cortex for α_1-ARs), frozen, and stored at −80 °C until the day of assay.

Tissue was homogenized in about 50 volumes of ice-cold 50 mM Tris-HCl buffer (pH 7.4) using an Ultra Turrax TP-1810 (2 × 20 s) and centrifuged at 50000*g* for 10 min (Beckman

model J-21B refrigerated centrifuge). The pellet was resuspended in the same volume of fresh buffer, incubated at 37 °C for 10 min, and centrifuged again at 50000*g* for 10 min. The pellet was then washed once by resuspension in fresh buffer and centrifuged as before. The pellet was then resuspended in the appropriate incubation buffer (50 mM Tris-HCl, pH 7.7, containing 10 μM pargyline and 4 mM $CaCl_2$ for 5-HT_{1A} receptors; 50 mM Tris-HCl, pH 7.7, containing 10 μM pargyline and 0.1% ascorbic acid for α_1-ARs; 50 mM Tris-HCl, pH 7.1, containing 10 μM pargyline, 120 mM NaCl, 5 mM KCl, 2 mM $CaCl_2$, 1 mM $MgCl_2$, and 0.1% ascorbic acid for D_1 and D_2 receptors) just before the binding assay.

Binding assays were done as previously described.[38] Briefly, the following incubation conditions were used. 5-HT_{1A}: [^{3}H]-8-OH-DPAT (sp act. 157 Ci/mmol, NEN) final concentration 1 nM, 30 min, 25 °C (nonspecific binding, 5-HT 10 μM). D_1: [^{3}H]-SCH23390 (sp act. 71.1 Ci/mmol, NEN) final concentration 0.4 nM, 15 min, 25 °C (nonspecific binding, (−)-*cis*-flupentixol 10 μM). D_2: [^{3}H]spiperone (sp act. 19.0 Ci/mmol, NEN) final concentration 0.2 nM, 15 min, 37 °C (nonspecific binding, (−)-sulpiride 100 μM). α_1-ARs: [^{3}H]prazosin (sp act. 71.8 Ci/mmol, NEN) final concentration 0.2 nM, 30 min, 25 °C (nonspecific binding, phentolamine 3 μM).

Incubations were stopped by rapid filtration under vacuum through GF/B filters which were then washed with 12 mL (4 × 3 times) of ice-cold 50 mM Tris-HCl (pH 7.4) using a Brandel M-48R apparatus and counted in 4 mL of Filter Count (Packard) in a LKB 1214 RACKBETA liquid scintillation spectrometer with counting efficiency of about 60%. Dose−inhibition curves were analyzed by the "Allfit" program to obtain the concentration of unlabeled drugs that inhibited ligand binding by 50%.[39] The K_i values were derived from the IC_{50} values.[40]

Molecular Modeling. All calculations and graphic manipulations were performed on an SGI Origin300 server and an Octane 12K workstation by means of the Catalyst (version 4.8) and Cerius^2 (version 4.8.1) software packages.

All the compounds used in this study were built using the 2D−3D sketcher of Catalyst. A representative family of conformations was generated for each molecule using the poling algorithm and the "best quality conformational analysis" method. Conformational diversity was emphasized by selection of the conformers that fell within 20 kcal/mol above the lowest energy conformation found. The Compare/Fit command has been used to predict activity values of the studied compounds. Particularly, the Best Fit option has been selected which manipulates the conformers of each compound to find, when possible, different mapping modes of the ligand within the model. Affinity values for test set compounds were calculated by the program on the basis of the following equation:

$$\text{affinity} = 10^{-(\text{Fit}+\text{Intercept})}$$

where the term Fit quantifies how well each compound was able to fit the pharmacophoric features, while the term Intercept represents the intercept of the regression equation on the *y* axis estimating the affinity of training set compounds. Further details can be found on the Accelrys Web site: http://www.accelrys.com/doc/life/catalyst49/help/catalyst/VHToolsmenu.doc.html#306504.

The Compare/Fit command has also been used to perform molecular alignment of compounds to be submitted to QSAR analysis. In detail, RN5 was fitted onto the pharmacophoric model and its best fitted conformation was used as a template to align compounds **21**−**40** through the Best Fit option. Next, for each molecule in such an alignment, the atomic partial charges were calculated by means of the Mopac software and AM1 approximation, as implemented in the InsightII (version 2000.1) software package. Molecules with their charges were imported in Cerius^2 to perform a QSAR analysis based on the genetic function approximation (GFA) algorithm. The GFA parameter set used in this study was based on an initial population of 100 equations that were evolved through 20 000 crossover operations. To evaluate if the GFA algorithm reached convergence, a plot of the number of times a variable has been used versus the number of crossovers (variable usage graphic) was analyzed. In particular, when the frequency of descriptor usage remained unaltered, it suggested the optimal value of crossover operations (∼20 000 in this study). Moreover, the fact that descriptors found in the best final QSAR equations (reported in Table 3) were the most frequently represented in this graphic indicated that the GFA algorithm reached convergence.

During GFA analysis, only linear polynomial terms were allowed to be included in the final models. Default values of mutation and smoothing parameters were kept, and the least-squares method was used for regression.

Supporting Information Available: Elemental analysis data. This material is available free of charge via the Internet at http://pubs.acs.org.

References

(1) Hieble, J. P.; Bondinell, W. E.; Ruffolo, R. R. α- and β-Adrenoceptors: From the Gene to the Clinic. 1. Molecular Biology and Adrenoceptor Subclassification. *J. Med. Chem.* **1995**, *38*, 3415−3444.

(2) Ruffolo, R. R., Jr.; Bondinell, W.; Hieble, J. P. α- and β-Adrenoceptors: From the Gene to the Clinic. 2. Structure−Activity Relationships and Therapeutic Applications. *J. Med. Chem.* **1995**, *38*, 3681−3716.

(3) Ford, A. P. D. W.; Williams, T. J.; Blue, D. R.; Clarke, D. E. α_1-Adrenoceptor Classification: Sharpening Occam's Razor. *Trends Pharmacol. Sci.* **1994**, *15*, 167−170.

(4) Hieble, J. P.; Bylund, D. B.; Clarke, D. E.; Eikemburg, D. C.; Langer, S. Z.; Lefkowiz, R. J.; Minneman, K. P.; Ruffolo, R. R. International Union of Pharmacology. X. Recomandation for Nomenclature of α_1-Adrenoceptors: Consensus Update. *Pharmacol. Rev.* **1995**, *47*, 267−270.

(5) Zhong, H.; Minneman, K. P. α_1-Adrenoceptor Subtypes. *Eur. J. Pharmacol.* **1999**, *375*, 261−276.

(6) Flavahan, N. A.; Vanhoutte, P. M. α-Adrenoceptor Subclassification in Vascular Smooth Muscle. *Trends Pharmacol. Sci.* **1986**, *7*, 347−349.

(7) Muramatsu, I.; Ohmura, T.; Kigoshi, S.; Hashimoto, S.; Ospita, M. Pharmacological Subclassification of α_1-Adrenoceptors in Vascular Smooth Muscle. *Br. J. Pharmacol.* **1990**, *99*, 197−201.

(8) Grassi, G. Sympathetic Deactivation as a Goal of Nonpharmacologic and Pharmacologic Antihypertensive Treatment: Rationale and Options. *Curr. Hypertens. Rep.* **2003**, *5*, 277−280.

(9) Vaughan, E. D. Jr. Medical Management of Benign Prostatic Hyperplasia. Are Two Drugs Better Than One? *N. Engl. J. Med.* **2003**, *349*, 2449−2451.

(10) Hancock, A. H. α_1 Adrenoceptor Subtypes: A Synopsis of Their Pharmacology and Molecular Biology. *Drug Dev. Res.* **1996**, *39*, 54−107.

(11) Trumpp-Kallmayer, S.; Hoflack, J.; Bruinvels, A.; Hibert, M. Modeling of G-Protein-Coupled Receptors: Application to Dopamine, Adrenaline, Serotonin, Acetylcholine, and Mammalian Opsin Receptors. *J. Med. Chem.* **1992**, *35*, 3448−3462.

(12) Barbaro, R.; Betti, L.; Botta, M.; Corelli, F.; Giannaccini, G.; Maccari, L.; Manetti, F.; Strappaghetti, G.; Corsano, S. Synthesis, Biological Evaluation, and Pharmacophore Generation of New Pyridazinone Derivatives with Affinity towards α_1- and α_2-Adrenoceptors. *J. Med. Chem.* **2001**, *44*, 2118−2132.

(13) (a) Betti, L.; Floridi, M.; Giannaccini, G.; Manetti, F.; Strappaghetti, G.; Tafi, A.; Botta, M. α_1-Adrenoceptor Antagonists. 5. Pyridazinone-arylpiperazines. Probing the Influence on Affinity and Selectivity of Both *ortho*-Alkoxy Groups at the Arylpiperazine Moiety and Cyclic Substituents at the Pyridazinone Nucleus. *Bioorg. Med. Chem. Lett.* **2003**, *13*, 171−173. (b) Betti, L.; Corelli, F.; Floridi, M.; Giannaccini, G.; Maccari, L.; Manetti, F.; Strappaghetti, G.; Botta, M. α_1-Adrenoceptor Antagonists. 6. Structural Optimation of Pyridazinone-Arylpiperazines. Study of the Influence on Affinity and Selectivity of Cyclic Substituents at the Pyridazinone Ring and Alkoxy Groups at the Arylpiperazine Moiety. *J. Med. Chem.* **2003**, *46*, 3555−3558.

(14) Carroll, W. A.; Sippy, K. B.; Esbenshade, T. A.; Buckner, S. A.; Hancock, A. A.; Meyer, M. D. Two Novel and Potent 3-[(*o*-Methoxyphenyl)piperazinylethyl]-5-phenylthieno[2,3-d]pyrimidine-2,4-diones Selective for the α_{1D} Receptor. *Bioorg. Med. Chem. Lett.* **2001**, *11*, 1119−1121.

(15) Barlocco, D.; Cignarella, G.; DalPiaz, V.; Giovannoni, M. P.; De Benedetti, P. G.; Fanelli, F.; Montesano, F.; Poggesi, E.; Leonardi, A. Phenylpiperazinylalkylamino Substituted Pyridazinones as Potent α_1 Adrenoceptor Antagonists. *J. Med. Chem.* **2001**, *44*, 2403−2410.

(16) Chern, J.; Tao, P.; Wang, K.; Gutcait, A.; Liu, S.; Yen, M.; Chien, S.; Rong, J. Studies on Quinazolines and 1,2,4-Benzothiadiazine 1,1-Dioxides. 8.[1,2] Synthesis and Pharmacological Evaluation of Tricyclic Fused Quinazolines and 1,2,4-Benzothiadiazine 1,1-Dioxides as Potential α_1-Adrenoceptor Antagonists. *J. Med. Chem.* **1998**, *41*, 3128−3141.
(17) Russo, F.; Romeo, G.; Guccione, S.; De Blasi, A. Pyrimido[5,4-*b*]indole Derivatives. 1. A New class of Potent and Selective α_1 Adrenoceptors Ligands. *J. Med. Chem.* **1991**, *34*, 1850−1854.
(18) Meyer, M. D.; Carrol, W. A. Piperazinyl Pyrimidine Dione Compounds Selective for Adrenoceptors. U.S. 6,153,614, November 28, 2000.
(19) Rogers, D.; Hopfinger, A. J. Application of Genetic Function Approximation to Quantitative Structure−Property Relationships. *J. Chem. Inf. Comput. Sci.* **1994**, *34*, 854−866.
(20) Rogers, D. Some Theory and Examples of Genetic Function Approximation with Comparison to Evolutionary Techniques. In *Genetic Algorithms in Molecular Modeling*; Devillers, J., Ed.; Academic Press: London, 1996; pp 87−107.
(21) Furneaux, R. H.; Tyler, P. C. Improved Synthesis of 3*H*,5*H*Pyrrolo-[3,2-*d*]pyrimidines. *J. Org. Chem.* **1999**, *64*, 8411−8412.
(22) Chen, N.; Lu, Y.; Gadamasetti, K.; Hurt, C. R.; Norman, M. H.; Fotsch, C. A Short, Facile Synthesis of 5-Substituted 3-Amino-1*H*-pyrrole-2-carboxylates. *J. Org. Chem*. **2000**, *65*, 2603−2605.
(23) Norman, M. H.; Chen, N.; Han, N.; Liu, L.; Hurt, C. R.; Fotsch, C. H.; Jenkins, T. J.; Moreno, O. A. Bicyclic Pyridine and Pyrimidine Derivatives as Neuropeptide Y Receptor Antagonists. WO 9940,091, August 12, 1999.
(24) Norman, M. H.; Chen, N.; Chen, Z.; Fotsch, C.; Hale, C.; Han, N.; Hurt, R.; Jenkins, T.; Kincaid, J.; Liu, L.; Lu, Y.; Moreno, O.; Santora, V. J.; Sonnenberg, J.; Karbon, W. Structure−Activity Relationships of a Series of Pyrrolo[3,2-*d*]pyrimidine Derivatives and Related Compounds as Neuropeptide Y5 Receptor Antagonists. *J. Med. Chem.* **2000**, *43*, 4288−4312.
(25) Goetz, A. S.; King, H. K.; Ward, S. D. C.; True, T. A.; Rimele, T. J.; Saussy, D. L., Jr. BMY 7378 Is a Selective Antagonist of the D Subtype of α_1-Adrenoceptor. *Eur. J. Pharmacol*. **1995**, *272*, R5−R6.
(26) Yocca, F. D.; Hyslop, D. K.; Smith, D. W.; Maayani, S. BMY 7378, a Buspirone Analogue with High Affinity, Selectivity and Low Intrinsic Activity at the 5-HT_{1A} Receptor in Rat and Guinea Pig Hippocampal Membranes. *Eur. J. Pharmacol*. **1987**, *137*, 293−294.
(27) Russell, R. K.; Press: J. B.; Rampulla, R. A.; McNally, J. J.; Falotico, R.; Keiser, J. A.; Bright, D. A.; Tobia, A. Thiopene Systems. 9. Thienopyrimidinedione Derivatives as Potential Anthypertensive Agents. *J. Med. Chem*. **1988**, *31*, 1786−1793.
(28) Romeo, G.; Russo, F.; Guccione, S. Heterocyclic Systems Containing the Pyrimido-2,4-dione Ring as Selective Ligands for the α_1-Adrenoceptors. *Farmaco* **1995**, *6*, 471−477.
(29) Cerius[2] (version 4.8.1), Catalyst (version 4.8), and InsightII (version 2000.1) softwares are distributed by Accelrys, Scranton Road, San Diego, CA.
(30) Fan, Y.; Shi, L. M.; Kohn, K. W.; Pommier, Y.; Weinstein, J. N. Quantitative Structure−Antitumor Activity Relationships of Camptothecin Analogues: Cluster Analysis and Genetic Algorithm-Based Studies. *J. Med. Chem*. **2001**, *44*, 3254−3263.
(31) Gokhale, V. M.; Kulkarni, V. M. Understanding the Antifungal Activity of Terbinafine Analogues Using Quantitative Structure−Activity Relationship (QSAR) Models. *Bioorg. Med. Chem*. **2000**, *8*, 2487−2499.
(32) Lee, K. W.; Briggs, J. M. Comparative Molecular Field Analysis (CoMFA) Study of Epothilones-Tubulin Depolymerization Inhibitors: Pharmacophore Development Using 3D QSAR Methods. *J. Comput.-Aided Mol. Des.* **2001**, *15*, 41−55.
(33) Wang, S.; Sakamuri, S.; Enyedy, I. J.; Kozikowski, A. P.; Zaman, W. A.; Johnson, K. M. Molecular Modeling, Structure−Activity Relationships and Functional Antagonism Studies of 4-Hydroxy-1-methyl-4-(4-methylphenyl)-3-piperidyl 4-Methylphenyl Ketones as a Novel Class of Dopamine Transporter Inhibitors. *Bioorg. Med. Chem.* **2001**, *9*, 1753−1764.
(34) Internal or standard cross-validation in GFA encompasses only the optimization of regression coefficients but does not encompass the optimization of the choice of molecular descriptors.
(35) Kier, L. B.; Hall, L. H. An Electrotopological-State Index for Atoms in Molecules. *Pharm. Res.* **1990**, *7*, 801−807.
(36) Hall, L. H.; Mohney, B.; Kier, L. B. The Electrotopological State: An Atom Index for QSAR. *Quant. Struct.−Act. Relat.* **1991**, *10*, 43−51.
(37) Procedures involving animals and their care were conducted in conformity with the institutional guidelines that are in compliance with national (D.L. n. 116, G.U., Suppl. 40, February 18, 1992) and international laws and policies (EEC Council Directive 86/609, OJ L 358, 1, December 12, 1987; Guide for the Care and Use of Laboratory Animals, U.S. National Research Council, 1996).
(38) Caccia, S.; Confalonieri, S.; Guiso, G.; Bernasconi, P.; Cagnotto, A.; Skorupscka, M.; Mennini, T. Brain Uptake and Distribution of the Potential Memory Enhancer CL 275,838 and Its Main Metabolites in Rats: Relationship between Brain Concentrations and in Vitro Potencies on Neurotransmitter Mechanisms. *Psychopharmacology* **1994**, *115*, 502−508.
(39) De Lean, K. W.; Munson, P. J.; Rodbard, D. Simultaneous analysis of families of sigmoidal curves: application to bioassay, radioligand assay, and physiological dose−response curves. *Am. J. Physiol.* **1978**, *235*, E97−E102.
(40) Cheng, Y.; Prusoff, W. H. Relationship between the Inhibition Constant (K_i) and the Concentration of Inhibitor Which Causes 50 per Cent Inhibition (IC_{50}) of an Enzymatic Reaction. *Biochem. Pharmacol.* **1973**, *22*, 3099−3108.

JM040870H